An Analysis of CFAR Thresholds and Scale Factors with Window Effects in Pulse Compression

Kyoungchan Seo, Junho Song, Jong-Mann Kim, and Jegyung Son
Agency for Defense Development (ADD)
Daejeon, South Korea
{kyoungchan, alway5, jman95, jgs}@add.re.kr

***Abstract*—This paper presents an analysis of the window effects on the constant false alarm rate (CFAR) techniques. In this research, the scale factors for the robust CFAR detectors, which are not explicitly defined by theoretical equations, are derived by utilizing the Monte Carlo method. To ensure the reliability of the implemented Monte Carlo simulations, we compare the scale factors between the theory and the simulations in cell averaging-CFAR (CA-CFAR). The need for a credible adjustment of the scale factor to achieve a consistent false alarm probability is confirmed through simulations that investigate noise distributions and CFAR thresholds with various windows in pulse compression.**

Keywords—radar signal processing, robust CFAR techniques, pulse compression, Monte Carlo simulation, scale factor, false alarm probability, noise distribution, target detection.

I. INTRODUCTION

Recently, the radar field has been continuously researched in various IT areas such as aircraft, ships, automobiles, and weather forecasting [1]. The fundamental principle of the radar systems is to emit signals and then detect the target's position through a series of signal processing including pulse compression, coherent integration (CI) / non-coherent integration (NCI), and threshold calculation using the received signals reflected back from the targets. The received signals contain not only target signals but also interference signals, such as noise and clutter signals from unintended targets. Therefore, it is necessary to establish thresholds to distinguish target signals from these interferences, and a prominent technique for determining such threshold values is constant false alarm rate (CFAR).

Through CFAR techniques, a constant false alarm probability can be maintained according to system requirements, and the basic CFAR architecture is cell averaging CFAR (CA-CFAR) [2]. In addition, various forms of robust CFAR techniques have been developed, such as greatest ordered CA-CFAR (GOCA-CFAR) [3], Smallest Ordered CA-CFAR (SOCA-CFAR)[4], censored-CFAR (CS-CFAR) [5], [6], trimmed mean-CFAR (TM-CFAR) [7], and ordered static-CFAR (OS-CFAR) [8], [9] are used to cope with non-homogeneous environments including clutter edge false alarm and mutual target masking. These methodologies involve calculating relevant statistics for each approach and refining the statistics with scale factors to accomplish the false alarm rate of system requirements.

Nevertheless, in radar operation, variations in the number of pulses during NCI aimed at achieving a consistent detection range within the beam grid, along with changes of windows in pulse compression designed to enhence distance resolution and signal-to-noise ratio (SNR), can influence the received signal data used in CFAR thresholds calculation process, leading to fluctuating false alarm rates that differ from the system requirements.

This study employs Monte Carlo techniques to decide suitable scale factors for different robust CFAR methods, ensuring the required false alarm probability in compliance with system specifications. Furthermore, the research examines how changes in noise distribution resulting from various window variations in pulse compression. The validity of this analysis is demonstrated through the comprehensive comparison of noise distributions and CFAR thresholds, considering the application of scale factors.

II. SYSTEM MODEL

Fig. 1 shows the system block diagram considered in this paper. We consider a radar signal processing system which incorporates two main steps: the first step utilizes noise-only inputs for deriving CFAR scale factors, and the second step involves mixed inputs of noise and transmitted signals to calculate CFAR thresholds by multiplying the scale factors. The detection results can be attained when the signals after Doppler processing exceeds the CFAR thresholds in Fig. 1.

A. Signal Model

In this system, the received signal is written as

$$y(t) = s(t) + z(t), \tag{1}$$

where $s(t)$ is a transmitted signal with Linear Frequency Modulation (LFM) waveform [10], and $z(t)$ is a complex Gaussian noise at time t.

B. Various Windows in Pulse Compression

Pulse compression is commonly used to achieve high range resolution with wide pulses in the radar operation. However, an assortment of windows can be employed to alleviate the distortion of waveform edges in such pulse compression by the spectral leakage for the finite DFT extent. The signal after this processing is represented as

$$p(t) = y(t) \circledast \left[r(t) w_{pc}(t)\right]^*, \tag{2}$$

where $r(t)$ is a reference signal like the transmitted signal, and $w_{pc}(t)$ is the window waveform in pulse compression. $\circledast$ denotes a convolution operator, and $(\cdot)^*$ denotes a complex conjugate.

We utilize the three windows in Fig. 2: 1) Rectangular window, 2) Hamming window [11], 3) Blackman-Harris window [12]. Note that normalizing the window power to 1 is

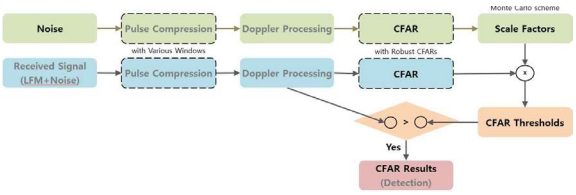

Fig. 1. An illustration of the system block diagram.

crucial to reduce the scaling effect caused by the windows. This normalization allows straightforward signal comparison while preserving the total signal energy.

C. Doppler Processing and CFAR schemes

The signal after Doppler processing is expressed as

$$D(e^{jw}) = \mathcal{F}[p(t)w_{dp}(t)], \tag{3}$$

where $w_{dp}(t)$ is the window waveform in Doppler processing, and $\mathcal{F}(\cdot)$ denotes the fast Fourier transform (FFT) operator. In this study, we conduct the Doppler processing with the Chebyshev window.

Then, CFAR techniques are facilitated to determine the thresholds for discriminating between targets and noise. Further description about CFAR schemes is provided in the next section.

III. Robust CFAR Algorithms

CFAR is a valuable algorithm for analyzing a series of data across diverse fields. The fundamental common structure of CFAR involves extracting a statistic from the reference cells surrounding a cell under test (CUT), and then comparing the CUT with the threshold value derived from the statistic. While a variety of CFAR methods exist in detail, the following six algorithms are implemented as depicted in Fig. 3.

A. CA-CFAR

CA-CFAR is one of the most foundational techniques among the CFAR algorithms. Initially, a statistical value associated with a CUT can be obtained by taking the average from reference cells. Subsequently, this computed statistic is

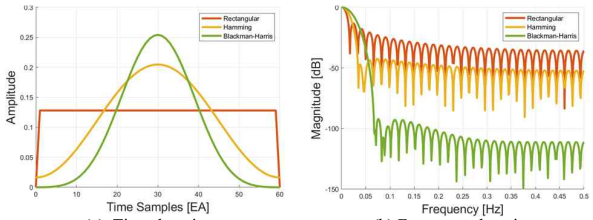

(a) Time domain (b) Frequency domain

Fig. 2. Characteristics of three windows in pulse compression.

multiplied by the scale factor of CA-CFAR to derive a threshold in contrast with the CUT in accordance with Fig. 3(a).

B. GOCA-CFAR

GOCA-CFAR exhibits similarities with CA-CFAR, albeit with distinct differences. In Fig. 3(b), statistics are categorized into two types: one is the statistic from lagging reference cells and the other is the statistic from leading reference cells. Among the two statistics, the larger one is selected for determining a threshold. Accordingly, GOCA-CFAR can be useful in addressing the conditions with clutter edge false alarm in clutter boundaries by sharply increasing the interference values [13].

C. SOCA-CFAR

The majority of algorithmic sequence in SOCA-CFAR corresponds to that of GOCA-CFAR with the exception of choosing the smaller one between the two statistics as shown in Fig. 3(c). SOCA-CFAR can be beneficial to restrain the mutual target masking in cases that there are other target signals within the reference cells [13].

D. CS-CFAR

CS-CFAR is a strategy that the values of reference cells are sorted in ascending order, and then statistics are computed by taking the average of the remaining part excluding the top N_L largest values in the fashion of Fig. 3(d). Through the removal of the top elements, we can fulfill the effect of moderating the environment as mutual target masking [13] like in SOCA-CFAR.

E. TM-CFAR

TM-CFAR in Fig. 3(e) is an approach that evaluates the mean using the reference cell data after eliminating the N_S smallest elements as well as the top N_L largest elements, differing from CS-CFAR. Therefore, by employing TM-CFAR, it is possible to prevent not only mutual target masking but also clutter edge false alarm [13].

F. OS-CFAR

The procedure of OS-CFAR is comparable to that of TM-CFAR except for the aspect of retaining only the k^{th} element and discarding the rest. In other words, OS-CFAR is a skill that selects the k^{th} element in the sorting data of reference cells. Thus, there is no necessity for the computation process for the acquisition of statistics in OS-CFAR. Similarly to TM-CFAR, OS-CFAR can yield a limiting influence on both mutual target masking and clutter edge false alarm [13].

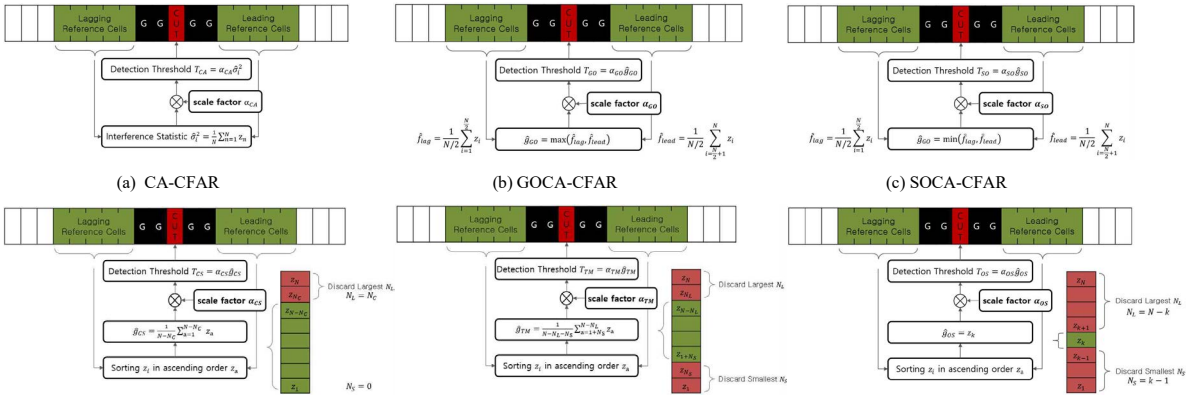

(a) CA-CFAR (b) GOCA-CFAR (c) SOCA-CFAR

(d) CS-CFAR (e) TM-CFAR (f) OS-CFAR

Fig. 3. Block structures of six CFAR procedures.

IV. SIMULATION ANALYSIS

In this section, an analysis of the simulation results is furnished, taking into account different configurations of CFAR techniques and three windows in pulse compression. To this end, we determine the appropriate scale factors at the desired false alarm probability by comparing Monte Carlo simulation with the theory related to false alarm probability.

The CFAR parameters used in the simulation are as follows. The size of reference window cells is $N = 40$, and guard sizes G is 3 on the both sides of a CUT. $N_S = 14$ and $N_L = 36$ in CS-CFAR and TM-CFAR, and $k = 30$ in OS-CFAR.

A. Scale Factors in Theory and Monte Carlo simulation

Given a scale factor and the size of reference window cells, a closed-form formula exists to calculate the false alarm probability in CA-CFAR as follow [13].

$$P_{fa} = \left[1 + \frac{\alpha_{CA}}{N}\right]^{-N}, \tag{4}$$

which means that α is a scale factor. Using (4), we get

$$\alpha_{CA} = N\left[P_{fa}^{-\frac{1}{N}} - 1\right]. \tag{5}$$

In contrast, such a closed-form expression is notably absent in other CFARs. Hence, the scale factors in the most cases of CFARs should be estimated with Monte Carlo simulation as presented in Fig. 4.

We can see that scale factors in the rectangular window are identical to those of the theory in Fig. 4(a). In instances where the rectangular window is employed, it is resulting in a mere change in size by normalizing the window power to 1. Consequently, with demonstrating the equivalence of scale factor results of the theory and the simulation, we establish the credibility of Monte Carlo simulation in this paper. Additionally, Fig. 4(b), Fig. 4(c), and Fig. 4(d) show the relationship between scale factors and false alarm probabilities in the three windows, respectively.

Exploiting the data from Fig. 4, the scale factors with false alarm probability of 10^{-4} are organized in Table 1. A discernible trend of increasing scale factors in Table 1 can be identified in the order of rectangular, Hamming, and Blackman-Harris window in the similar manner to Fig. 4(a). The scale factors form Table 1 are utilized in the subsequent simulations.

B. CFAR Thresholds with Target signals

Fig. 5 represents the CFAR thresholds with the scale factors adjusted to $P_{fa} = 10^{-4}$ for the situation involving a signal target. In Fig. 5(a), sharp spikes due to pulse compression contribute to clutter edge false alarms across all CFARs. Fig. 5(b) showcases the alleviating effect of Hamming window, resulting in the mitigation of false alarms in the majority of CFARs except for SOCA-CFAR. Blackman-Harris window offers the potential to further alleviate the signals around the target including SOCA-CFAR in Fig. 5(c). Nonetheless, this modification sharpens the waveform, causing threshold fluctuations in the vicinity of the target area.

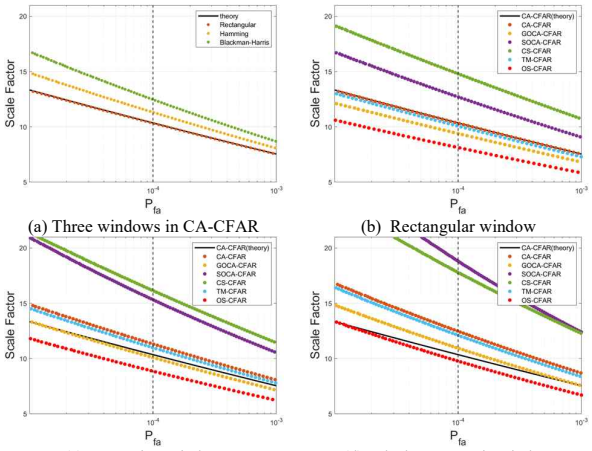

(a) Three windows in CA-CFAR (b) Rectangular window

(c) Hamming window (d) Blackman-Harris window

Fig. 4. Scale factor versus false alarm probability.

TABLE I. SCALE FACTORS IN MONTE CARLO SIMULATION

CFAR Type	Window Type		
	Rectangular	***Hamming***	***Blackman-Harris***
CA-CFAR	10.3	11.3	12.5
GOCA-CFAR	9.4	10.1	10.9
SOCA-CFAR	12.7	15.3	18.8
CS-CFAR	14.8	16.1	17.8
TM-CFAR	10.1	11.0	12.1
OS-CFAR	8.1	8.9	9.8

The CFAR thresholds for the case of two targets are depicted in Fig. 6. CA-CFAR and GOCA-CFAR demonstrate a challenging characteristic of struggling to handle mutual target masking in Fig. 6(a). Conversely, SOCA-CFAR, CS-CFAR, and TM-CFAR exhibit a remarkable capability in managing the neighboring targets, and it is established that OS-CFAR is minimally affected by adjacent targets with the derivation of smooth thresholds.

Our simulations confirm that clutter edge false alarm is prevented by eliminating the N_S smallest values within the reference window during the threshold calculation. Correspondingly, removing the N_L largest values mitigates mutual target masking. Among robust CFAR methods, it is evident that OS-CFAR approach is most effective in reducing the number of false alarms in heterogeneous scenarios.

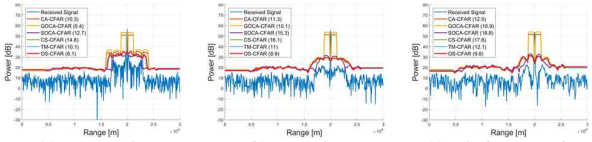

(a) Rectangular (b) Hamming (c) Blackman-Harris

Fig. 5. CFAR thresholds in the single target scenario.

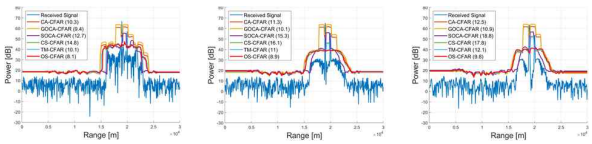

(a) Rectangular (b) Hamming (c) Blackman-Harris

Fig. 6. CFAR thresholds in the scenario of dual targets.

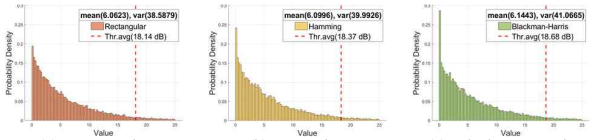

(a) Rectangular (b) Hamming (c) Blackman-Harris

Fig. 7. Noise distibution after Doppler processing and threshold average.

C. Comparison of the Noise Distributions

In order to analyze the window effects applied to pulse compression about CFAR thresholds and scale factors, we conduct an investigation into the noise distribution as illustrated in Fig. 7. Examining the probability density distributions, it is observed that a more growth in variances and the threshold averages of CA-CFAR with the red dashed lines because the mean values and the prevalence of smaller data values increase in the sequence of rectangular window, Hamming window, and Blackman-Harris window. The simulation results indicate that CFAR process and the noise component are influenced by the distinct characteristics of the main lobe width of and the side lobe magnitude in each window. As a result, the adjustment of the CFAR scale factor is essential for the purpose of acquiring CFAR thresholds that match the specified false alarm probability in accordance with the specifications.

V. Conclusion

In this paper, we validate the credibility of our simulations through a comparative analysis between scale factors derived from theoretical consideration and those obtained via Monte Carlo simulations. Moreover, Monte Carlo simulations offer suitable scale factors for robust CFAR techniques and diverse window configurations in pulse compression, especially in situations where theoretical derivation is not feasible. The simulation results suggest the necessity of appropriately adjusting the scale factors to ensure a consistent false alarm probability when applying different windows in radar signal processing. Further work involves extending the study to estimate efficient parameters including N_S, N_L in TM-CFAR and k in OS-CFAR under heterogeneous environments.

References

[1] B. R. Mahafza and A. Z. Elsherbeni, MATLAB Simulaions for Radar Systems Design, CRC, London, 2004.

[2] H. M. Finn and R. S. Johnson, "Adaptive detection mode with threshold control as a function of spatially sampled clutter-level estimates," Rca Rev., pp. 414–464, September 1968.

[3] V. G. Hansen and J. H. Sawyers, "Detectability loss due to "gratest of" selection in a cell-averaging CFAR," IEEE Trans. Aerosp. Electron. Syst., vol. 16, no. 1, pp. 115–118, January 1980.

[4] G. V. Trunk, "Range resolution of targets using automatic detectors," IEEE Trans. Aerosp. Electron. Syst., vol. 14, no. 5, pp. 750–755, September 1978.

[5] J. T. Rickard and G. M. Dillard, "Adaptive detection algorithms for multiple-target situations," IEEE Trans. Aerosp. Electron. Syst., vol. 13, no. 4, pp. 338–343, July 1977.

[6] J. A. Ritcey, "Performance analysis of the censored mean-level detector," IEEE Trans. Aerosp. Electron. Syst., vol. 22, no. 4, pp. 443–454, July 1986.

[7] P. P. Gandhi and S. A. Kassam, "Analysis of CFAR processors in nonhomogeneous background," IEEE Trans. Aerosp. Electron. Syst., vol. 24, no. 4, pp. 427–445, July 1988.

[8] H. Rohling, "Radar CFAR thresholding in clutter and multiple target situations," IEEE Trans. Aerosp. Electron. Syst., vol. 19, no. 4, pp. 608–621, July 1983.

[9] H. Rohling, "New CFAR-precessor based on an ordered statistic," in Proc. IEEE Int. Radar Conf., Arlington, VA, pp. 271–275, 1985.

[10] J. R. Klauder, A. C. Price, S. Darlington, and W. J. Albersheim, "The theory and design of chirp radars," Bell Syst. Tech. J., vol. 34, pp. 745–808, 1960.

[11] A. V. Oppenheim, W. S. Ronald, and R. B. John, Discrete-Time Signal Processing, Upper Saddle River, NJ, Prentice Hall, 1999.

[12] F. J. Harris, "On the use of windows for harmonic analysis with the discrete fourier transform," Proc. IEEE, vol. 66, pp. 51–83, 1978.

[13] M. A. Richards, J. A. Scheer, and W. A. Holm, Principles of Modern Radar, vol. 1: Basic Principles, SciTech Publishing, Edisson, NJ, 2010